

# Electroplating of Stainless Steel

L. Philippe,\* C. Heiss, and J. Michler

EMPA, Swiss Federal Laboratories for Materials Testing and Research, Laboratory of Mechanics and Nanostructures, Feuerwerkerstrasse 39, CH-3602 Thun, Switzerland

Received December 17, 2007. Revised Manuscript Received February 15, 2008

A novel procedure for the electrochemical deposition of a Fe–Ni–Cr alloy was investigated on stainless steel and copper substrates. The alloy contains approximately 56–58% Fe, 26–28% Ni, and 14–16% Cr in weight, close to that of a standard stainless steel 316. We show that it is possible to produce a thick (up to 23  $\mu\text{m}$ ) and stressless deposit of the alloy. The first aim of this work was the development of a stable electrolyte containing Fe(II), Ni(II), and Cr(III) with a suitable chromium complexing agent. The influence of process parameters (temperature, current density, agitation of the electrolyte, and the nature of the cathode) upon the deposition was investigated. A particular study of the chromium complexation was performed. The composition and surface state of thick deposits prepared using either dimethylformamide (DMF) or glycine as a chromium complexant were compared and revealed that glycine used as a chromium(III) complexing agent, gives highly reproducible deposits with stable compositions and suitable mechanical properties and surface state. The mechanical and corrosion properties of the developed alloy were determined and compared with a standard 316 stainless steel reference sample. Finally, the successful deposition of the alloy inside a mold using the UV-LIGA technique shows the ability of the procedure to produce micro/nanostructures with highly desirable properties such as biocompatibility, durability, and resistance to corrosion.

## Introduction

Stainless steel is a widely used alloy in different areas, thanks to its good corrosion resistance, mechanical, and magneto-resistive properties.<sup>3–5</sup> The good resistance of steel in aggressive media and its biocompatibility would make the alloy an excellent candidate for developing cheap biodevices<sup>6</sup> if stainless steel could be synthesized by electrodeposition. Electrodeposited Fe–Ni–Cr alloys, with a composition near that of steel<sup>1,2</sup> would allow advantage to be taken of the aforementioned properties of the alloy and at the same time produce electroformed structures with high aspect ratios and complex shapes by utilizing a LIGA procedure. Electrodeposition of binary to quaternary alloys such as Fe–Ni,<sup>7</sup> Fe–Cr,<sup>8</sup> FeNiCr,<sup>1,2</sup> and Fe–Ni–Cr–Mo,<sup>9</sup> have been reported in the literature but were mainly limited to producing thin layers (principally for decorative purposes). However, these reports are important in terms of description of anomalous codeposition processes occurring with the ferromagnetic elements.

In addition to the complexity of producing a ternary alloy by electrochemical means, the presence of chromium in high quantity in the deposit is a challenge by itself, for different reasons. First of all, chromium(III) aqua-species,  $\text{Cr}(\text{H}_2\text{O})_6^{3+}$ , being a very strong Lewis acid, undergoes a rapid olation reaction between unprotonated forms in aqueous electrolytes, annihilating chromium deposition.<sup>10</sup> To prevent this phenomenon, we should investigate chromium complexation with ligands that are at the same time a better complexing agent than water and that are easily released from chromium(III) during the deposition process. Several complexing agents are candidates, and results from ethylenglycol,<sup>11</sup> DMF,<sup>1</sup> citrate,<sup>9</sup> glycine,<sup>8,12–15</sup> acetate,<sup>16</sup> formate,<sup>17</sup> and hydroxylamine phosphate/hydrazine<sup>18</sup> have been reported.

Additionally, the presence of chromium in the alloy (despite its anticorrosive properties) decreases the quality of the structure of the surface by the formation of cracks.<sup>19</sup> Because of these cracks, Ni–Cr systems can only have a limited thickness.<sup>19</sup> The increase of internal stress inside an alloy containing chromium<sup>15</sup> causes a finer grain structure,

\* Corresponding author. E-mail: laetitia.philippe@empa.ch.

- (1) El-Sharif, M. R.; Watson, A.; Chisholm, C. U. *Trans. IMF* **1988**, *66*, 34.
- (2) El-Sharif, M. R.; MacDougall, J.; Chisholm, C. U. *Trans. Inst. Met. Finish.* **1999**, *77* (4), 139.
- (3) Erik. Oberg, *Machinery's Handbook*, 25th ed.; Industrial Press Inc.: New York, 1996; p 411.
- (4) Harris, T. E.; Whitney, G. M.; Croll, I. M. *J. Electrochem. Soc.* **1995**, *142*, 1031.
- (5) Andricacos, P. C.; Robertson, N. *IBM J. Res. Dev.* **1998**, *42*, 671.
- (6) Romankiw, L. T. *Electrochim. Acta* **1997**, *42*, 2985.
- (7) Myung, N. V.; Park, D.-Y.; Yoo, B.-Y.; Sumodjo, P. T. A. *J. Magn. Mater.* **2003**, *265*, 189.
- (8) Wang, F.; Watanabe, T. *Mater. Sci. Eng., A* **2003**, *349*, 183.
- (9) Dolati, A. G.; Ghorbani, M.; Afshar, A. *Surf. Coat. Technol.* **2003**, *166*, 105.

- (10) Smith, A. M.; Watson, A.; Vaughan, D. H. *Trans. Inst. Met. Finish.* **1993**, *71*, 106.
- (11) Aoyagi, J.; Kowaka, M. *J. Surf. Finish. Soc. Jpn.* **1989**, *40*, 453.
- (12) Masanobu, I. *Electrodeposition of Iron and Iron Alloys*. In *Modern Electroplating*, 4th ed.; John Wiley & Sons: New York, 2000; p 461.
- (13) Prabhuram, J.; Manoharan, R. *J. App. Electrochem.* **1998**, *28*, 935.
- (14) Lallemand, F.; Ricq, L.; Bercot, P.; Pagetti, J. *Electrochimica Acta* **2002**, *47*, 4149.
- (15) Ghorbani, A.; Zad, I.; Dolati, A.; Ghasempour, R. *J. Alloys Compd.* **2005**, *386*, 43.
- (16) Arthanareeswaran, G.; Thanikaivelan, P.; Jaya, N.; Mohan, D.; Raajenthiren, M. *J. Hazard. Mater.* **2007**, *B139*, 44.
- (17) Baral, A.; Engelken, R. *J. Electrochem. Soc.* **2005**, *152* (7), C504.
- (18) Survilinié, S.; Jasulaitiene, V.; Nivinskiene, O.; Cesuniene, A. *Appl. Surf. Sci.* **2007**, *253*, 6738.
- (19) Bahrololoom, E.; Hoveidaei, A. *Surf. Eng.* **1999**, *15* (6), 502.

which is normally attributed to an increase in the nucleation rate of the deposits. The grain refinement has, however, a positive consequence, as it makes the alloy harder, which is beneficial for certain applications. The problem of cracks was already met in various metallic electrodeposited alloys.<sup>19</sup> In order to overcome this problem and especially in the case of chromium containing alloys, the employment of an organic additive, generally that contains a sulfur atom, such as saccharine<sup>20–22</sup> to reduce the stress has already been described and may help to get a better deposit quality. On the other hand, these additives are known to prevent the formation of a passivated oxide layer at the surface, thereby decreasing the corrosion resistance of the alloy.<sup>22,23</sup>

Furthermore, the reduction of water into hydrogen (whose reductive potential is close to that of reduction of Cr(III) to Cr(II) and to Cr(0)) runs with very low overpotential on transition metal<sup>24</sup> deposits and leads to free hydrogen and hydroxide anions. This reaction of reduction of water decreases the cathode efficiency and the hydroxide increases the pH, which precipitates the iron and the nickel as their insoluble hydroxides. Also, partial reduction of Cr(III) to Cr(II) species may occur at the decreasing potential during the plating.<sup>1</sup> The precipitation of Cr(III) species into the deposits is also a source of problems.<sup>18</sup>

The complexity of chromium's electrochemical behavior, coupled with the already difficult task of controlled anomalous codeposition of ternary alloys is a challenge by itself. Indeed, the control of such deposits is not only interesting fundamentally but has great potential for applications in micro/nanotechnology.

In this study, a novel electrolytic bath allowing the deposition of Fe–Ni–Cr alloys with a composition approaching that of a standard stainless steel 316, with good mechanical properties for a deposit up to 23  $\mu\text{m}$  thick has been developed. Deposition variables that were investigated included chromium complexing agent, temperature, current density, and degree of agitation of the bath. We found that two complexing agents for chromium, namely, glycine and DMF, can give deposits of the right composition and thickness. Surface state and mechanical and corrosion properties of the developed alloys were determined and tested. Finally, we demonstrate the possibility of depositing the alloy in a micromold through the UV-LIGA technique, which opens a wide range of applications for the alloy. The best deposits were obtained using glycine as chromium complexing agent. We obtained in a reproducible way a stressless alloy, with a composition containing 56–58% Fe, 26–28% Ni, and 14–16% Cr.

## Experimental Section

**(1) Electrochemical Deposition.** A conventional three-electrode cell system was used in order to realize the electrodeposition. A

**Table 1. Composition of the Electrolyte for Fe–Ni–Cr Alloy Electrodeposition, Excluding the Complexing Agent of Chromium**

electrolyte composition	quantity (mol/L)
$\text{CrCl}_3 \cdot 6\text{H}_2\text{O}$	0.4
$\text{NiCl}_2 \cdot 6\text{H}_2\text{O}$	0.2
$\text{FeCl}_2 \cdot 4\text{H}_2\text{O}$	0.03
$\text{NH}_4\text{Cl}$	0.5
$\text{NaCl}$	0.5
$\text{H}_3\text{BO}_3$	0.15

copper or 316 steel cathode and a graphite high density anode were used. The potential was measured against a standard calomel electrode.

The plating bath was prepared by dissolving chemical reagents (Table 1) in deionized water. The chemical grade reagents consisted of chromium(III) chloride hexahydrate and the chromium complexing agent dissolved in deionized water and heated to 80 °C for 30 min. The nickel(II) sulfate hexahydrate, ferrous chloride tetrahydrate, boric acid as nickel complexing agent, ammonium chloride as antioxidant and sodium chloride were dissolved in deionized water and heated to 30–40 °C for 30 min. Then, the two baths were mixed thoroughly. During deposition, the electrolyte temperature was under cryostat controlled.

The different complexant species studied for chromium are noted in Table 2.

Before the electrodeposition, the cathode substrates were polished mechanically to 2000 mesh grit and then polished using 0.3  $\mu\text{m}$  alumina powder. Just before plating, the cathode substrates were washed successively in acetone, ethanol, isopropanol, and diluted sulfuric acid and briefly dried using an argon flow. The surface area of the cathode was 0.95  $\text{cm}^2$ . The cathode agitation was performed via a Rotating Disk Electrode (RDE) of the cathode at 250 rpm together with a constant agitation of the bath through a magnetic stirring of the electrolyte at the bottom of the electrochemical cell.

Before any experiment on a new bath, several blank experiments were run.

**(2) Deposit Characterization.** Depth profiles of elemental composition of the deposits were obtained by Glow Discharge Optical Emission Spectroscopy (GDOES).<sup>25</sup> The morphology of the deposits was inspected using optical and scanning electron microscopy. The corrosion behavior of the alloys was characterized by carrying out potentiodynamic polarization measurements on selected deposits with an exposed area of 0.785  $\text{cm}^2$  in a 1 M NaCl solution at a controlled temperature of 25 °C. Open circuit potentials (OCP) were measured versus an Ag/AgCl electrode. A platinum circular grid was used as support electrode. The applied potential range was between –1 and 2 V with a scan rate of 5 mV/s.

Nanoindentation tests were performed using a MTS Nanoindenter XP with a Berkovich diamond tip. For each sample, several load-displacement curves with a peak load of 10 mN were measured and an average curve was used to calculate hardness and Young's modulus according to the Oliver and Pharr procedure.<sup>26</sup> The peak load was chosen such that the maximum indentation depth remained below 10% of the total film thickness.

**(3) Resist Patterning.** A plating-base was vapor-deposited on a polished silicon wafer, consisting of 20 nm thick titanium (adhesion layer) and 100-nm thick copper (seed layer), respectively. Prior to the photoresist deposition, a commercial layer (Omnicoat, Microliography Chemical Corporation, MCC), was applied to the substrate surface for improving adhesion and stripping behavior of

(20) Kounchenova, M.; Raichevski, G.; Vitkova, S. T. *Surf. Technol.* **1987**, *31*, 137.

(21) El Sherik, A. M.; Erb, U. *J. Mater. Sci.* **1995**, *30*, 5743.

(22) Smith, R. S.; Godyski, L. E.; Lloyd, J. C. *J. Electrochem. Soc.* **1961**, *108*, 996.

(23) Frenkel, G. S.; Brusica, V.; Schad, R. G.; Chang, J.-W. *Corros. Sci.* **1993**, *35*, 63.

(24) Srimathi, S. N.; Mayanna, S. M. *Mater. Chem. Phys.* **1984**, *11*, 351.

(25) Payling, R.; Michler, J.; Aeberhard, M. *Surf. Interface Anal.* **2002**, *33*, 472.

(26) Oliver, W. C.; Pharr, G. M. *J. Mater. Res.* **2004**, *19*, 3–20.

**Table 2. Chromium(III) Complexing Agents Studied in Molar Equivalent with Chromium(III)**

complexing agent molar eq. referred with Cr	<i>N,N</i> -dimethylformamide (C <sub>3</sub> H <sub>7</sub> NO) solvent	formic acid (HCOOH) solvent	acetic acid (CH <sub>3</sub> COOH) solvent	glycine (H <sub>2</sub> NCH <sub>2</sub> COOH) 1.0–2.0
--	---	--------------------------------	---	---

the photoresist. A negative SU8–2035 (MCC) photoresist of high viscosity was then applied to a thickness of 50- $\mu\text{m}$  by a spin-coating process. After the baking processes, the polymer-coated substrates was exposed to a UV source by using a maskless lithographic tool (model SF-100, Intelligent Micropatterning). The technology utilizes reflective micro optics to allow direct circuit image projection onto a substrate surface. The desired pattern is designed using conventional drawing software. Resist development consisted of an immersion process in the alkaline commercial developer from MCC. The bath composition is described in Table 2 and used glycine as chromium complexant. In addition, some organic additives (saccharine, sodium dodecyl sulfate (SDS), and Zonyl commercial Dupont-10022D) at a concentration of 1.0 g/L were tested.

During electroplating, the temperature was kept at 15 °C with 10 A/dm<sup>2</sup>; a deposition rate of approximately 10  $\mu\text{m}/\text{h}$  was observed with a deposition yield of nearly 100%. After plating, the stripping of the photoresist was performed in the commercial MCC stripper solvent.

## Results

**(1) Parameter Screening.** The study reported here was performed using glycine as complexing agent for chromium. The same investigation using DMF has also been done and resulted in the same trends in terms of the influence upon the composition of the deposit.

*Chemical Composition of the Cathode.* Two different cathodes were used: steel-316L and elemental copper. Both had the same surface area (0.95 cm<sup>2</sup>) and were polished and prepared using the same procedure. For the same experimental conditions, we obtained the same alloy composition on both substrates; this is contrary to potentiostatic deposition where the applied potential depends on the nature of the substrate.<sup>2</sup> Good throwing and covering power has been obtained from the galvanostatic process for both substrates. However, at high current densities, the deposits on a 316L cathode were more heterogeneous (full of cracks) and physically less stable. Furthermore, at the beginning of the deposition, close to the substrate–deposit interface, a small difference in composition is found between each of the substrates. For depositions above 1  $\mu\text{m}$  thick, the compositions are very similar for the two substrates. The greater physical instability is observed only at the beginning of the deposition as evidenced by GDOES spectra. This shows that for thin layer deposition, the substrate influences greatly the growth mode and therefore composition of the deposit. On the other hand, with thicker deposits, the influence of the substrate becomes negligible. In the presented work, copper substrates were always used.

*Temperature.* Figure 1a displays the composition of the deposit as a function of the electrolytic bath temperature for a current density of 10 A/dm<sup>2</sup> under controlled laminar flow convection produced by the RDE rotation; Figure 1b gives the same set of experiments with natural convection.

From Figure 1a, it is interesting to note that the electrolyte temperature range between 10 and 25 °C and at 10 A/dm<sup>2</sup> seems to allow a deep decomplexation of the chromium.

Indeed, the elemental Cr is found at an amount of 10% in the deposit and is not linked with deposition of other elements (such as C and O) that remains very low (less than 1%). For temperatures greater than 30 °C, the concentration decreases to less than 5% and at temperatures greater than 35 °C, the chromium concentration in the deposit falls down to less than 2%. On the other hand, the proportion of nickel increases with temperature whereas the concentration of iron remains constant. The same tendencies were already reported in the literature.<sup>24</sup> Finally the deposition rate increases logically with temperature, which is explained by the thermal agitation that favors the evolution of hydrogen, increasing the rates of both reduction reactions of water and metal salts in general. The decreasing amount of chromium in the deposit indicates that the reduction of chromium Cr<sup>3+</sup> into Cr<sup>2+</sup> as a first reduction step is in close competition with that of water, as suggested by their respective standard

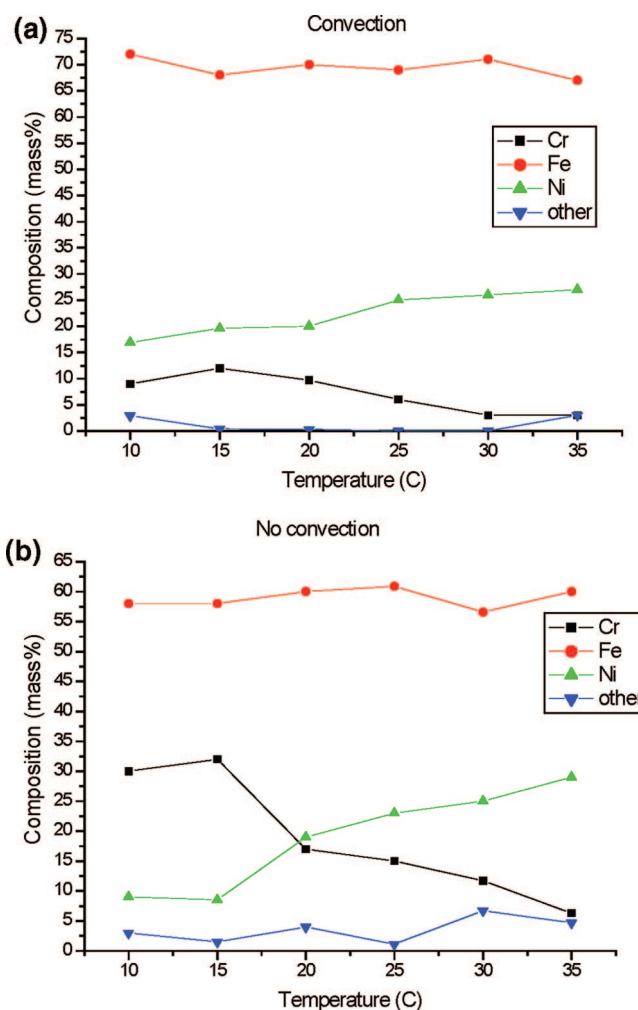


**Figure 1.** Elemental composition of the deposit measured at a depth of 5  $\mu\text{m}$  for a deposit of 10  $\mu\text{m}$  thick analyzed by GDOES as a function of the temperature applied during the galvanostatic deposition for a current density of 10 A/dm<sup>2</sup>: (a) with forced convection on the cathode, (b) with no convection.



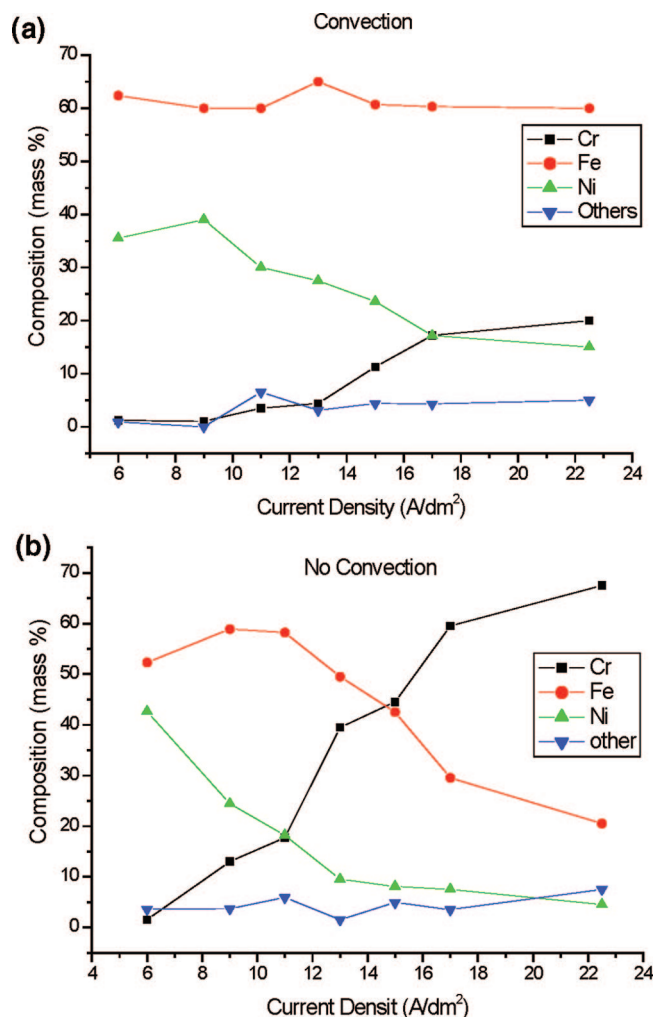


**Figure 2.** Elemental composition of the deposit measured at a depth of 5  $\mu\text{m}$  for a deposit of 10  $\mu\text{m}$  thick analyzed by GDOES as function of the current density applied during the galvanostatic deposition for a temperature of 20  $^{\circ}\text{C}$ : (a) with forced convection on the cathode, (b) with no convection.

reduction potentials.<sup>27</sup> Indeed, reduction of water is known to be kinetically spontaneous on iron-group metals and this despite the use of boric acid. This implies that there is some applied current consumed by hydrogen formation.<sup>24,28</sup> However, when providing a sufficient convection on the surface a constant hydrogen evolution was possible and the concentration of H in the deposit was below 0.5%. In conclusion, an electrolyte temperature of 20 to 25  $^{\circ}\text{C}$  under controlled convection for a polarization current of 10  $\text{A}/\text{dm}^2$  gives the best results in term of deposit aspect ratio, composition and thickness.

**Current Density.** The elemental composition of the deposit as a function of the current density applied for controlled convection of the electrolyte is given in Figure 2a. All the experiments were performed in a galvanostatic mode with a range of current densities (CD) from 6 to 22  $\text{A}/\text{dm}^2$ . The corresponding potentials were varied from  $-1.9$  to  $-2.5$  V. Results for the CD variation were all performed at a temperature of 20  $^{\circ}\text{C}$ .

As can be seen from Figure 2a, the composition of the deposit is logically strongly linked to the current density value. All the measurement series showed that increasing the current density results in a higher chromium content in the deposit. This is in agreement with the general rule that during electrochemical deposition, an increase in CD favors the proportion of the less noble metal, in this case, chromium, inside the electrodeposited material.<sup>29</sup> On the other hand, the proportion of nickel shows a decrease with the increase in CD. This is due to the fact that deposition of nickel is under diffusion control.<sup>24</sup> For a temperature of 20  $^{\circ}\text{C}$ , as shown in Figure 2a, and for a current density of 12.6  $\text{A}/\text{dm}^2$ , a deposit with a composition of 12–15% chromium, 51–53% iron, and 20–30% nickel and with a thickness of 19.2  $\mu\text{m}$  was successfully obtained.

At a controlled current density, the subsequent stability of the potential plays an important role for the stability of the composition. The concentration of the three metallic species in the diffusion layer evolves through the deposit, thus changing the potential value. As the potential slightly decreases with time during the experiments, the deposit generally contains more chromium at the beginning than at the end of the deposition process. This variation can reach more than 5%. Under potentiostatic control, the concentration was more constant during plating. However, this method was not used, as more Cr(II) is produced that deposits in the alloy, decreasing its thickness and quality as has been previously reported.<sup>1</sup>

**Agitation.** The influence of the convective flow above the cathode on the elemental composition can be seen by comparing panels a and b in Figure 1, and panels a and b in Figure 2, respectively. From both comparisons (CD and temperature), it is clear that a laminar flow due to the cathode rotation allows a relative stability in the composition of the deposit, especially for species controlled in diffusion mode, as is here the case for nickel, which will benefit from a thinner diffusion layer induced by convection in contrast to chromium. As such, we notice that under a controlled convection of 250 rpm at 15  $^{\circ}\text{C}$  with 10  $\text{A}/\text{dm}^2$ , less than 10% of chromium was measured in the deposit for 20% nickel and 68% Fe, whereas in the absence of stirring of the cathode, more than 30% of chromium is deposited and the Ni and Fe percentages are much lower than previously with convection. Additionally, it was noticed that a deposit obtained without convection contained a higher amount of impurities, mainly oxygen and carbon that were always correlated with each other. At low temperatures and with a less vigorous stirring, a greater concentration of oxygen was measured following that of carbon, meaning that there are complexed chromium compounds in the deposit. Additionally, a strong increase in the concentrations of oxygen and hydrogen in the deposit was observed under strong stirring (above 250 rpm) and at high temperatures (above 30  $^{\circ}\text{C}$ ), because of favorable thermodynamic conditions for water reduction.

In conclusion, a 250 rpm agitation of the cathode, combined with a constant bath filtration and the use of a

(27) Song, Y. B.; Chin, D.-T. *Electrochim. Acta* **2002**, *48*, 349–356.

(28) Zech, N.; Landoldt, D. *Electrochim. Acta* **2000**, *45*, 3461.

(29) Lowenheim, F. A. *Modern Electroplating*, 3rd ed.; Wiley: New York, 1974; p 501.

magnetic stirrer at the bottom of the bath to ensure homogeneity of the electrolyte composition was finally selected to give the best aspect, composition, and thickness.

**(2) Complexation Study. Chromium Complexation and Oxygen Concentration.** As explained in the introduction, a good complexation of chromium in the bath is crucial for depositing stress free FeNiCr layers that are anticorrosive and in the correct stoichiometry. A systematic investigation of the potential of different ligands toward Cr(III) has been carried out and among them, DMF, glycine, and two acids (acetic and formic) were used for further analysis (see Table 2). The strength of the bond between the Cr(III) and the ligand dominates the potential needed to decomplex the system and allow deposition of chromium simultaneously with Ni and Fe. At each temperature, a limiting current density value (cell potential value) allowing the decomplexation of chromium is determined. As such, it has been measured that within the temperature range 20 to 25 °C, a current limit value of 5 A/dm<sup>2</sup> is required to break the bond between chromium species from DMF and therefore to deposit pure chromium inside the alloy; at the same temperature, the limit of decomplexation was of 10 A/dm<sup>2</sup> in the case of the glycine. On the other hand, for formic and acetic acids, a value of 50 A/dm<sup>2</sup> was needed to deposit chromium within the film. For any type of complexants used, we observe that oxygen is present only superficially and decreases very rapidly over a range of 0.5–0.8 μm. It has got two origins that depend on the reaction conditions. The first one is due to the presence of hydroxide anion originating from competitive reduction of water compared to chromium that is typically linked with the diminution of the deposit thickness.<sup>27</sup> The second source is due to adsorption of the chromium complexed species that is not decomplexed at low temperatures and low current densities, as testified by the curve of oxygen that follows the curve of carbon on the GDOES spectra. In addition, the oxygen is also due to native oxide films of the three metal species, as revealed in previous works by Raman spectroscopy for various Fe–Ni–Cr systems.<sup>31</sup>

**DMF as Complexant.** This complexing agent enables the inclusion of chromium in the deposit with low current densities: starting from 5 A/dm<sup>2</sup>, the deposit contains already chromium around 5%. This value is low, but better than that of all the other complexing agents tested at such a current density (see next paragraphs). This is due to the fact that DMF is a slower complexing agent compared to glycine.<sup>32</sup> The oxygen concentration drops to less than 1% after 0.3–0.5 μm.

The best composition is obtained with a current density around 7.5 A/dm<sup>2</sup>. In this condition, the composition is the following: 58% Fe, 22% Ni, and 17% Cr (Figure 3a). However, the surface of the deposit is highly cracked which prevents the practical use of this type of deposition. For higher current densities, the chromium concentration in-

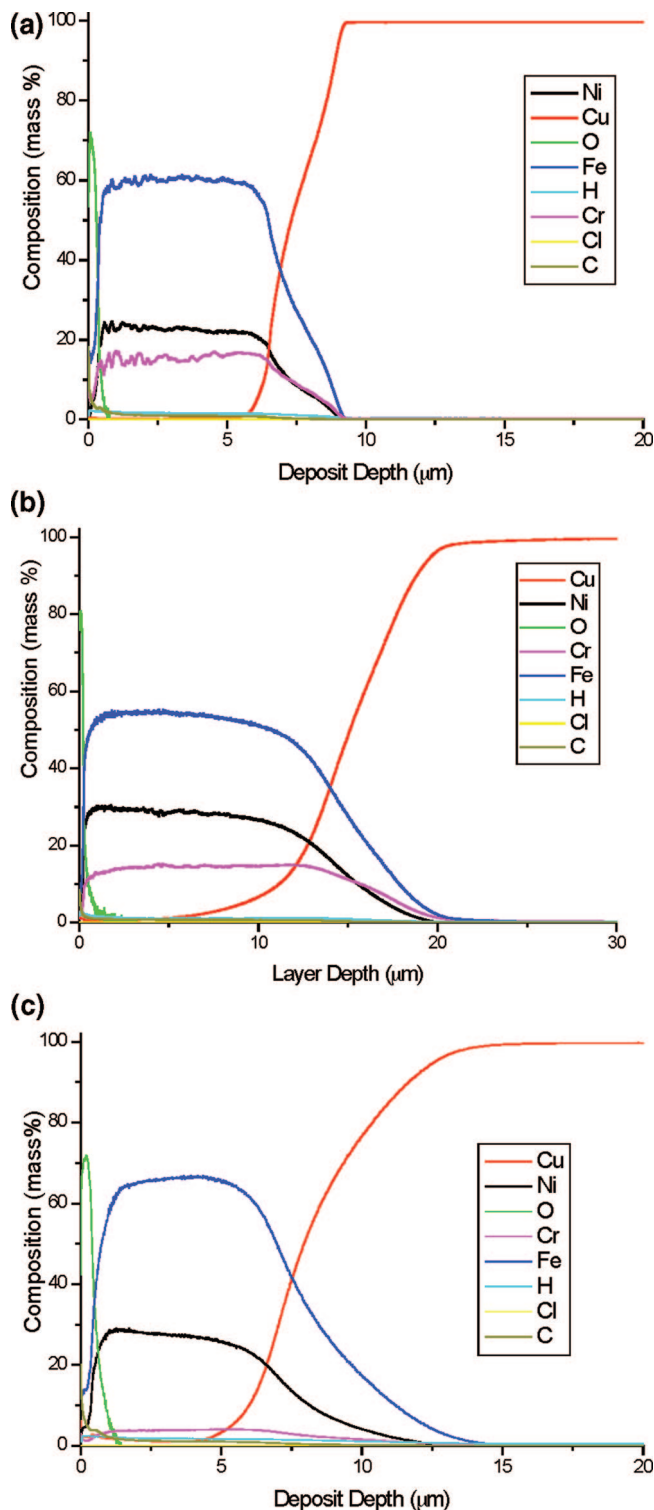


**Figure 3.** Elemental composition of the deposits made using different complexing agents for chromium analysed by GDOES: Figure 3(a) DMF, 3(b) glycine and 3(c) formic acid as complexants.

creases very fast, that of iron remains constant, and that of nickel decreases, as already discussed.

**Glycine as Complexant.** This complexing agent for chromium(III) used in a 1:1 mol equiv ratio gives the best deposits. As glycine complexes chromium(III) better than DMF, due to its delocalized nitrogen lone pair,<sup>32</sup> a greater current density or potential is necessary to get a given chromium concentration in the deposit. With this complexing

(30) Eisenberg, M.; Tobias, C. W.; Wilke, R. C. *J. Electrochem. Soc.* **1954**, *101*, 306.

(31) Oblonsky, L. J.; Devine, T. M. *Corros. Sci.* **1995**, *37*, 17.

(32) Geiger, D. K. *Coord. Chem. Rev.* **1997**, *164*, 261.

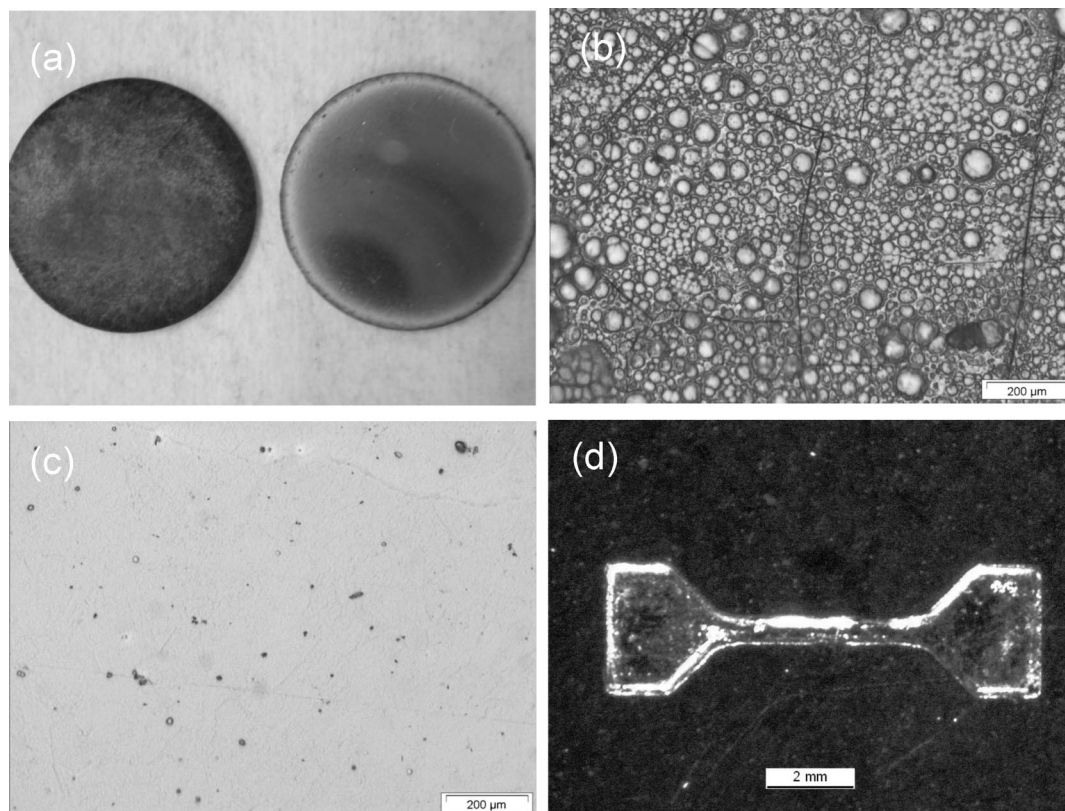


**Figure 4.** (a) Optical pictures of two FeNiCr surfaces of similar composition obtained with no complexation (left sample) and complexation with glycine (right image) of chromium. Details of the surface (b) with DMF and (c) by glycine; (d) optical picture of an electrodeposited FeNiCr microbar with  $9\ \mu\text{m}$  height obtained with the developed bath.

agent, it was not possible to obtain chromium in the deposit with a current density under  $5\ \text{A}/\text{dm}^2$ . Using potentiostatic mode, a minimum of  $1.9\text{--}2.0\ \text{V}/\text{ESH}$  is necessary. The best composition is obtained for a current density at  $10\ \text{A}/\text{dm}^2$ . For this condition, the composition is the following:  $56\text{--}58\%$  Fe,  $26\%$  Ni, and  $14\text{--}16\%$  Cr (Figure 3b). With this complexing agent, the oxygen concentration in the heart of the deposit is low (maximum  $1.5\%$ ). The current efficiency is higher using glycine, although the deposition time is longer, which allows an alloy to be built up with reduced internal stress and low hydrogen and oxygen content. A last but crucial advantage is that, for a similar chromium concentration in the deposit, the quality of the deposit surface is much better as revealed by optical microscopy (panels a and b in Figure 4 when using glycine instead of DMF).

**Acid Groups As Complexants.** Extremely strong complexing agents such as formic or acetic acids do allow chromium deposition at very high current densities ( $50\ \text{A}/\text{dm}^2$ ) but is strongly hindered by hydrogen reduction which renders a very low current efficiency for chromium deposition as already described by Song et al.<sup>27</sup> These CD values are directly linked with the potential useful to decomplex the chromium(III)-complexed species requested before chromium reduction. In this case, the current efficiency and the hydrogen content in the deposit are not satisfactory when one wants to proceed to the deposition of thin and stressless ternary alloys.

Concerning the complexant study, the use of glycine in a  $1.0\ \text{mol equiv}$  afforded the best quality of the deposit at a given concentration of chromium. Recently, a procedure for

preparing Fe–Cr–P alloys by electrodeposition reported that the chromium content is increased by using glycine as the complexing agent in a 2:1 ratio.<sup>35</sup> In our case, however, there was no significant increase of the chromium content using a higher amount of glycine and no amelioration of the deposits from 1:1 to 2:1 glycine: chromium ratio. Concentrations of oxygen, hydrogen, and carbon are identical and far below  $1\text{--}1.5\%$  in the deposit core. Oxygen naturally evolves at the anode and hydrogen, as partial reaction, at the cathode during the process. Whether glycine or DMF was used as the complexing agent, the same trends were observed for the influence of the temperature, the current density, or the stirring of the cathode upon deposit. The maximal thickness can not be higher than  $20\text{--}23\ \mu\text{m}$ , whatever the reaction time, because of the formation of Cr(II) species due to the decreasing potential<sup>1</sup> and the possible formation of a dimer species in the basic diffusion layer (due to the reduction of water) as recently reported for experiments run in sulfated medium.<sup>17</sup> When the reaction time is longer than 1600 to 2000 s, the deposits becomes black. Over a time of 2000–3000 s or longer, the thickness even decreases, showing a sensitivity of the alloy in the presence of an acidic medium and complexing agents. This is directly linked to the use of trivalent chromium and is a known limit for the production of thick coatings.<sup>27</sup> To summarize, the use of glycine as

(33) Wesley, W. *Trans. Inst. Met. Finish.* **1956**, *33*, 452.

(34) Barns, S. C. *J. Electrochemical Soc.* **1964**, *111*, 296.

(35) Li, B.; Lin, A.; Wu, X.; Zhang, Y.; Gan, F. *J. Alloys Compd.* **2008**, in press.



complexing agent allowed us to overcome the problem of sufficient deposition kinetics without producing cracked deposits.

**(3) UV-LIGA Assessment.** One main challenge in producing microstructures via an electrodeposition method is to overcome the filling difficulty inside a mask. For improving the wetting properties of the electrolyte, sulfur-containing organic additives were tested.

When using saccharine in the bath, neither improvements in the filling properties nor good aspect ratios (crack free surfaces) were obtained. However, using saccharine showed an increase of deposition time of the alloy and a certain stability of thickness to a maximum of 1–2  $\mu\text{m}$ ; with longer deposition time, no further deposition was possible. This deposition rate increase is known to be due to adsorption of SH-containing molecules which decreases the polarizability of the cathode and therefore stimulates the electrochemical discharge reaction by preventing proton or hydrogen adsorption.<sup>33,34</sup> However, the strong lamination of the deposit from 1  $\mu\text{m}$  thick only is a strong disadvantage of the wetting agent.

With sodium dodecyl sulfate (SDS), the composition changes notably: this additive favors the chromium rather than nickel and iron. This may be due to the fact that the competitive reduction of water into hydrogen is reduced as a consequence of the decrease of proton adsorption. This increase the deposition rate. As for saccharine, the build-up of thick deposits was not possible. Additionally, the deposit oxygen concentration is around 8% and is mainly due to the precipitation of the additive in the alloy during the plating. These changes of the composition may be attributed to the modification of the electrical conductivity of the plating bath and subsequently of the potential.

Wetting additives were subsequently not used during the deposition process. To improve the filling inside cavities, we produced a strong laminar flow about the patterned wafer was produced using a propeller rotation.<sup>36</sup> Figure 4d displays a typical microtensile bar of stainless steel obtained by electrodeposition and using the bath developed above. This shows the possibility of producing real micro pieces in stainless steel with a thickness up to 20  $\mu\text{m}$ . Although the surface is generally rough, there were no cracks on the surface. We have demonstrated the production of FeNiCr and further work on the wetting properties improvement is currently under investigation.

**(4) Mechanical and Corrosion properties.** Polarization curves are in shown in Figure 5a for deposits electrodeposited using glycine (FeNiCr\_A) and DMF (FeNiCr\_B) as complexing agents. For reference, a series of potentiodynamic curves were also performed on a stainless steel 316 (SS-316) substrate. As suspected, the stainless steel 316 presents more noble corrosion characteristics than the electrodeposited ones (see Table 3): lower current, lower pitting potential, and larger passivation range. However, it is interesting to see that the electrodeposited FeNiCr\_A and FeNiCr\_B exhibits very similar behavior to the standard SS-316 and confirms the very good corrosion resistance properties of the

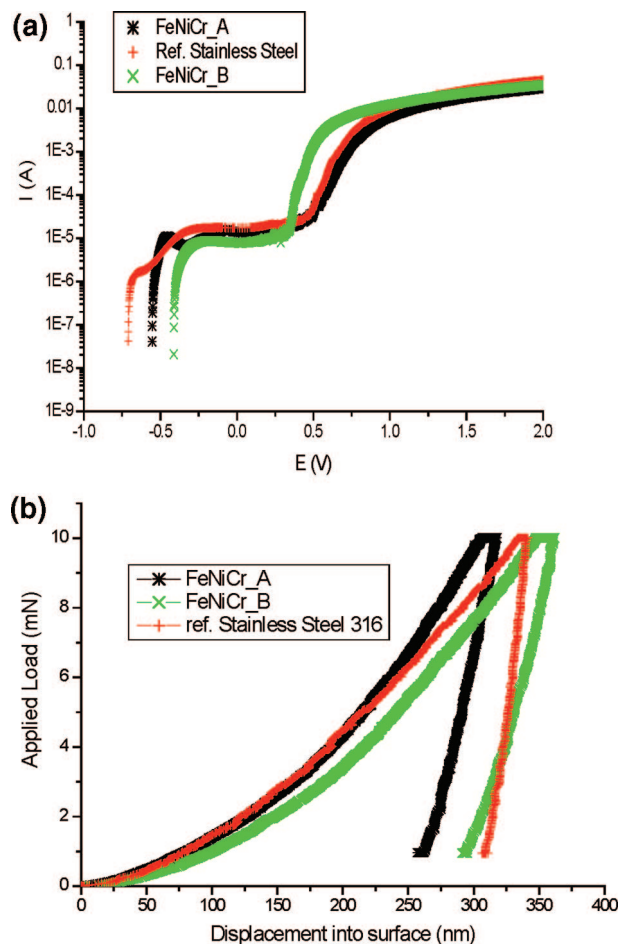


**Figure 5.** (a) Potentiodynamic polarization curves of electrodeposited FeNiCr A using glycine as complexant (FeNiCr\_A) or DMF (FeNiCr\_B) compared with standard stainless steel 316 as reference. (b) Typical Nanoindentation load-displacement curves comparing electrodeposited FeNiCr alloys using glycine as complexant (FeNiCr\_A) or DMF (FeNiCr\_B) compared with standard stainless steel 316 as reference.

**Table 3. Mechanical Properties of Ed. FeNiCr Complexed with Glycine (FeNiCr\_A) or DMF (FeNiCr\_B) Compared with Those of Stainless Steel 316, Measured by Nanoindentation Method and Corrosion Properties Measured by Polarization Method and Extracted from Figure 5a**

properties measured	FeNiCr_A	FeNiCr_B	stainless steel 316
Young's modulus (GPa)	123	107	198
hardness (GPa)	5.1	5.0	3.7
$I_{\text{corrosion}}$ (A/cm <sup>2</sup> )	$1.657 \times 10^{-5}$	$5.668 \times 10^{-6}$	$3.572 \times 10^{-6}$
$E_{\text{corrosion}}$ (V)	-0.413	-0.554	-0.623
$R_p$ ( $\Omega$ )	$1.767 \times 10^4$	$1.233 \times 10^4$	$1.124 \times 10^4$

electrodeposited alloys. It is possible, however, that for the FeNiCr\_B that is very much cracked, the corrosion properties of the alloy itself would be irrelevant for such a mechanically weak deposit.

Nanoindentation curves for the same deposits are given in Figure 5b and related mechanical properties in Table 3. The Young's moduli of the electrodeposited metals are lower compared to the reference stainless steel used. Hardness values are also different and higher for the electrodeposited materials. This might be due to the fact that the electrodeposited material has a finer grain size, although this was not investigated.

(36) Philippe, L.; Kern, P.; Michler, J. J. *Electrochem. Soc.* **2006**, *153*, C755.

### Discussion

We developed successfully a new method for the preparation of an electrodeposited Fe–Ni–Cr alloy with composition similar to that of a standard stainless steel 316. The thickness of the deposits are as much as 23  $\mu\text{m}$ . The major improvement is due to the employment of glycine as the chromium complexing agent. The influence of the electroplating parameters, such as the temperature, the current density or the stirring was successfully identified to reach the desired composition. High-quality deposits in terms of mechanical sustainability and surface aspect were obtained.

The strict control of all the physical parameters, such as temperature, current density, and agitation, was necessary to develop a reproducible technique. The smallest variation of one of the parameters greatly modified the composition of the deposited material. It was observed that temperature and agitation had the same effect on the chromium deposition. When either is too high, the hydrogen evolution from reduction of water was increased in place of the reduction of chromium(III). The increase in the current density, however, leads to an increase in the chromium content if the trivalent chromium is initially complexed with a suitable agent.

Compared to the El-Sharif modified protocol using DMF as complexing agent,<sup>1,2</sup> our protocol using glycine affords much better surface quality of the deposit (fewer cracks, images b and c in Figure 4). Other improvements such as high thickness, sufficient high deposition speed and low oxygen content were also achieved. The choice of chro-

mium(III) ligands was restricted to ligands that do not complex too strongly the chromium(III) ion and to ligands that do not undergo anodic oxidation. Isomers of picolinic and nicotinic acids that are known to be good labile complexants for chromium(III) were therefore unsuitable candidates.

The effects of the additives were various: saccharine and sodium dodecyl sulfate derivatives did not reduce the stress on the surface. They only modified its composition, increasing the chromium and oxygen concentrations and decreasing the iron and nickel concentrations. *Zonyl* derivatives allow deposition on tiny surfaces because of improved wetting properties, without anodization. They did not change the composition of the deposits, but they give more fragile deposits because of their increased oxygen concentration (up to around 8%).

Finally, corrosion and mechanical properties of the alloy were also tested and compared to a stainless steel 316. We show that the electrodeposited alloy has similar and very satisfactory properties that validate the interest in such bath development. The possibility of electrodeposition inside patterned surfaces for producing further MEMS and NEMS in stainless steel was demonstrated.

**Acknowledgment.** Financial support by the European commission in the Frame of the project MASMICRO is gratefully acknowledged. Special thanks go to C. Baret and H. Chaabouni for their help and collaboration in the success of this work. A big thank to James for the English correction.

CM703591N